



## Evidence of dynamic recrystallization in polar firn

Sepp Kipfstuhl,<sup>1</sup> Sérgio H. Faria,<sup>2</sup> Nobuhiko Azuma,<sup>3</sup> Johannes Freitag,<sup>1</sup> Ilka Hamann,<sup>1</sup> Patrik Kaufmann,<sup>4</sup> Heinrich Miller,<sup>1</sup> Karin Weiler,<sup>4</sup> and Frank Wilhelms<sup>1</sup>

Received 11 January 2008; revised 27 January 2009; accepted 4 February 2009; published 19 May 2009.

[1] Microstructural analyses have been performed on polar firn from the European Project for Ice Coring in Antarctica drilling site in Dronning Maud Land, Antarctica. The results derived from images of the firn structure in microscopic resolution indicate that dynamic recrystallization is active in firn at all depths, and it dominates the evolution of the microstructure when the firn density exceeds a critical value of  $730 \text{ kg/m}^3$  (overburden snow load  $\sim 0.2 \text{ MPa}$ ). At the firn-ice transition (density  $\sim 820 \text{ kg/m}^3$ ) the microstructure is characterized by many small grains and bulged or irregularly shaped grain boundaries. More than half of all grains show subgrain boundaries. Thus, strain-induced boundary migration is an essential feature to describe the irregular grain structure. In agreement with previous studies, significant grain growth has been observed with depth for the largest grains in the samples. However, our microscopic analysis reveals that the grain growth with depth in fact vanishes if all grains larger than  $65 \mu\text{m}$  in diameter are taken into account. This result reflects the fact that the growth of the largest grains is counteracted by grain size reduction by shrinking and subdivision of old grains, as well as production of new grains. Consequently, previous conclusions that grain growth in polar firn is essentially analogous to normal grain growth in metallic and ceramic sinters and that the stored strain energy is small in comparison with grain boundary energy can no longer be supported. Additionally, our observations show that the incipience of dynamic recrystallization in polar ice sheets is not as sensitive to temperature as supposed so far. A discussion of the change of the mean grain size due to the measuring technique is imperative.

**Citation:** Kipfstuhl, S., S. H. Faria, N. Azuma, J. Freitag, I. Hamann, P. Kaufmann, H. Miller, K. Weiler, and F. Wilhelms (2009), Evidence of dynamic recrystallization in polar firn, *J. Geophys. Res.*, 114, B05204, doi:10.1029/2008JB005583.

### 1. Introduction

#### 1.1. Background

[2] Recent grain size and lattice orientation analyses question the classical view of the onset of rotation recrystallization in the so-called normal grain growth regime in the upper hundreds of meters in polar ice sheets [Mathiesen *et al.*, 2004; Durand *et al.*, 2008]. In addition, deformation-related microstructural features like wavy grain boundaries, interlocking grain shapes, interacting subgrain boundaries observed already between 100 and 200 m depths in the EPICA Dronning Maud Land ice core [Kipfstuhl *et al.*, 2006; Faria *et al.*, 2009; Hamann *et al.*, 2009] provide evidence for dynamic recrystallization. These recent observations raise the question of which driving forces dominate

in the evolution of the microstructure and grain growth in firn and across the firn-ice transition. This is a particularly important question as the continuous increase of the average grain size with depth in firn, through the firn-ice transition, and in the upper hundreds of meters of an ice sheet still plays a central role in the discussion about the possible mechanisms controlling the deformation and recrystallization of polar ice [e.g., Gow and Williamson, 1976; Duval, 1985; Lliboutry and Duval, 1985; Wilson, 1986; Goldsby and Kohlstedt, 2001].

[3] On the basis of observations of Antarctic firn microstructure at South Ice and South Pole, Stephenson [1967] and Gow [1969] proposed a formula for the dynamic, isothermal grain growth in firn that is identical to the well-known law for grain growth in metals and ceramics under static conditions:

$$A = A_0 + K*t, \quad (1)$$

with  $A$  the mean crystal cross-sectional area,  $A_0$  the mean crystal cross-sectional area at time zero,  $K$  the growth rate and  $t$  time, i.e., the Normal Grain Growth (NGG) law. Accordingly, they interpreted the validity of the NGG formula as evidence that the driving force for grain growth in firn should be related to the curvature of the grain

<sup>1</sup>Alfred Wegener Institute for Polar and Marine Research, Bremerhaven, Germany.

<sup>2</sup>Section of Crystallography, GZG, University of Göttingen, Göttingen, Germany.

<sup>3</sup>Department of Mechanical Engineering, Nagaoka University of Technology, Nagaoka, Japan.

<sup>4</sup>Climate and Environmental Physics, Physics Institute, University of Bern, Bern, Switzerland.

boundaries, more precisely the reduction of the grain boundary free energy. In accordance with this reasoning, Duval [1985, p. 80] argued that the occurrence of normal grain growth in firn “implies that the strain energy is small in comparison with the grain boundary energy which drives grain growth.” Moreover, Duval and Castelnau [1995] concluded that a temperature of ca.  $-10^{\circ}\text{C}$  is crucial to initiate migration recrystallization. Since then, these two conclusions have become paradigmatic in specifying the deformation and recrystallization regimes in polar firn and ice.

[4] In this work we show that the evolution of the microstructure of polar firn is not adequately described by the concept of normal grain growth. We propose instead that the natural deformation of polar firn resembles the hot deformation of many metals and rocks. First, our microstructural analysis of Dronning Maud Land firn demonstrates that a new grain structure develops when the firn density reaches a critical value of  $730\text{ kg/m}^3$  (overburden snow load  $\sim 0.2\text{ MPa}$ ). The grain structure, initially of the “foam-type,” changes with depth to a much more complex one, rich in deformation-related features. This complete obliteration of the initial foam-like structure can only be explained by dynamic recrystallization, achieved by strain-induced boundary migration (SIBM), subdivision of old and formation of new grains. Temperature can obviously not be a crucial parameter for the onset of dynamic recrystallization, as the average temperature in Dronning Maud Land firn is ca.  $-45^{\circ}\text{C}$ .

[5] Second, in full accordance with our microstructural analysis we demonstrate the following.

[6] 1. The grain size distribution across the firn-ice transition is not stationary and thus not compatible with normal grain growth as previously proposed.

[7] 2. The interpreted grain growth depends on pragmatic assumptions concerning the handling of grain size data. If the whole grain size spectrum is taken into account, vanishing growth is revealed although the largest grains steadily increase their cross-sectional area. This behavior reflects dynamic equilibrium between grain growth and grain size reduction.

[8] 3. In contrast to normal grain growth, the strain energy stored in localized regions is a crucial driving force for grain boundary migration. Thus, SIBM in its various forms (rapid migration of old grain boundaries and nucleation of new grains) and rotation recrystallization play a fundamental role in the evolution of the firn microstructure.

## 1.2. Nomenclature

[9] It is always a dilemma to choose a consistent wording for discussing microstructure and recrystallization in minerals. This situation becomes even more difficult in the case of porous media, like firn. In an attempt to be systematic without being completely inconsistent with the cited literature, we employ here the following definitions. Firn is a porous, polycrystalline aggregate of snow/ice particles sintered together. Such particles may consist of single or polycrystalline domains called crystallites or grains. (By adopting the “particles-made-of-grains” convention we are tacitly adhering to the standard vocabulary of powder metallurgy and ceramics [Burke, 1959; Wilkinson and Ashby, 1975; Rice, 1998; Pan, 2003], while differing from

the “grains-made-of-crystals” convention employed in several firn studies [e.g., Stephenson, 1967; Gow, 1969].) Consequently, every grain may be characterized by its size, shape and lattice orientation. The term strain-induced recrystallization is used in reference to any recrystallization process driven by the stored strain energy, no matter whether new grains nucleate or not [cf. Cahn, 1974]. In particular, we shall be concerned here with the recrystallization mechanism named strain-induced boundary migration, or SIBM [see, e.g., Humphreys and Hatherly, 2004], which plays a fundamental role not only during the migration of old grain boundaries but also during the nucleation of new grains. As such, recrystallization phenomena involving nucleation of new grains will be included in the term nucleation recrystallization, or simply SIBM<sub>N</sub>, where the N subscript indicates that the migrating boundary belongs to a new grain or nucleus. Accordingly, for strain-induced recrystallization phenomena without nucleation of new grains we use the expression old grain recrystallization, or simply SIBM<sub>O</sub>, where the O subscript indicates that the migrating boundary belongs to an “old” grain originally present in the polycrystal (this corresponds to the process formerly called “grain boundary migration recrystallization” by Beck and Sperry [1950]). The partitioning of a grain into two or more subgrains by polygonization/tilting, twisting, microsheading or any similar intracrystalline process is named grain subdivision. Accordingly, the term rotation recrystallization is used in reference to the ultimate division of a grain into two or more grains by grain subdivision and subgrain rotation.

## 2. Methods

[10] Principles of the microstructure mapping method are described by Kipfstuhl *et al.* [2006]. Briefly, thermal grooves emerge on the surface of a carefully microtomed thin or thick section by enhanced sublimation at spots of high energy and defect concentration, like grain and subgrain boundaries or dislocation walls. Because the grooves scatter the transmitted or reflected light more than the ice matrix, they appear as gray or dark lines in the images (the deeper the groove, the darker the line). High-angle grain boundaries generally appear darker than subgrain boundaries or dislocation walls, which are usually relatively faint. Unlike the case of deep ice samples, we prepared only one surface and reduced the time for sublimation to the duration of the mapping itself ( $\sim 1\text{--}2\text{ h}$ , the time needed to take one or two sets of mosaic images). Mosaic images of the microstructure of the samples with typical dimensions of  $5\text{ cm}$  by  $10\text{ cm}$  are reconstructed from about 1500 single images. The resolution is  $3.25\text{ }\mu\text{m/pixel}$ .

[11] Three firn cores (B35, B36 and B37) drilled at Kohnen Station ( $75^{\circ}00'\text{S}$ ,  $00^{\circ}04'\text{E}$ ; the EPICA drill site in Dronning Maud Land, Antarctica) during the Austral field season 2005/2006 have been analyzed [EPICA Community Members, 2006]. The length of the cores are 30 m, 78 m and 124 m, respectively. Cutting of the cores and microstructure mapping was performed in the field within about 1–2 weeks after core retrieval. Mass density has been derived from weight, diameter and length of the cylindrical pieces (mostly 1 m long).

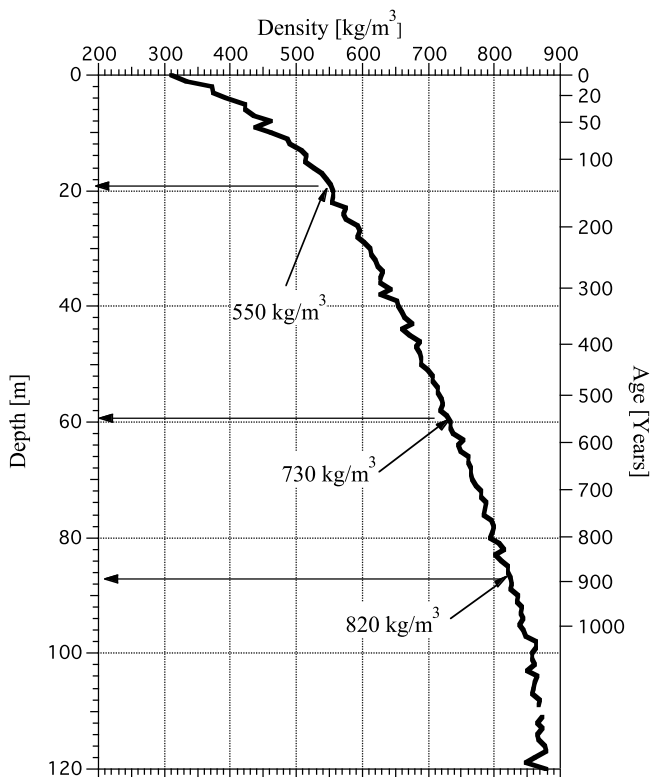


**Figure 1.** Composite density profile determined from diameter, length, and weight of single cores (core B36, 0–56 m; core B37, 56–120 m). Distance between both drill holes is about 10 m. The three critical firm densities of 550, 730, and 820  $\text{kg/m}^3$  after Maeno and Ebinuma [1983] are marked.

[12] Grain boundaries were extracted from the mosaic images applying the particle analysis routines provided by Object Image [Vischer *et al.*, 1994]. A disadvantage of Object Image is that the particle routines allow only a maximum image width of 4096 pixels. Therefore, grain sizes were determined from images reduced to 25% of their original size. Accordingly the resolution of the grain boundary network images is only 13  $\mu\text{m}/\text{pixel}$ . All grains with cross-sectional areas of more than 20 pixels, equivalent to the diameter of a circular area of about 65  $\mu\text{m}$ , were included for the grain size analysis. In order to analyze the subgrain structure, the number of grains showing subgrain boundaries was determined in an area of 13 mm by 13 mm (containing ca. 110–250 grains) of firm sections from every 10 m. Finally, the change in the grain structure was also analyzed through the measurement of the dihedral angles of ca. 200 grain boundary triple junctions in sections from 60 and 80 m depths.

### 3. Results and Discussion

#### 3.1. Density

[13] The density profile at the EPICA-DML drill site shows the normal behavior of cold dry firm on the plateau of large ice sheets (Figure 1). The critical mass densities of 550  $\text{kg/m}^3$ , 730  $\text{kg/m}^3$  and 820–840  $\text{kg/m}^3$  [Maeno and Ebinuma, 1983] are reached at ca. 20, 60 and 87 m depths,

respectively. The age at these depths is 140, 555 and 900 years. On the basis of a mean accumulation rate of 65  $\text{kg/m}^2\text{a}$  and assuming an average density of 300  $\text{kg/m}^3$  at the ice sheet surface, an annual layer thins from 216 mm at the surface to about 118, 89 and 79 mm at the depths of the three critical densities, respectively.

#### 3.2. Microstructural Analysis

[14] Figure 2 compares two sections from 60 m and 80 m depths with similar porosity. The differences in the grain structure and deformation-related features are evident. The equiaxed grains with gently curved or straight grain boundaries (foam-like structure) in Figure 2a are characteristic of a recrystallization regime in which grain boundary area is minimized, e.g., grain boundary migration driven by the interface free energy. In clear contrast, the grain structure in

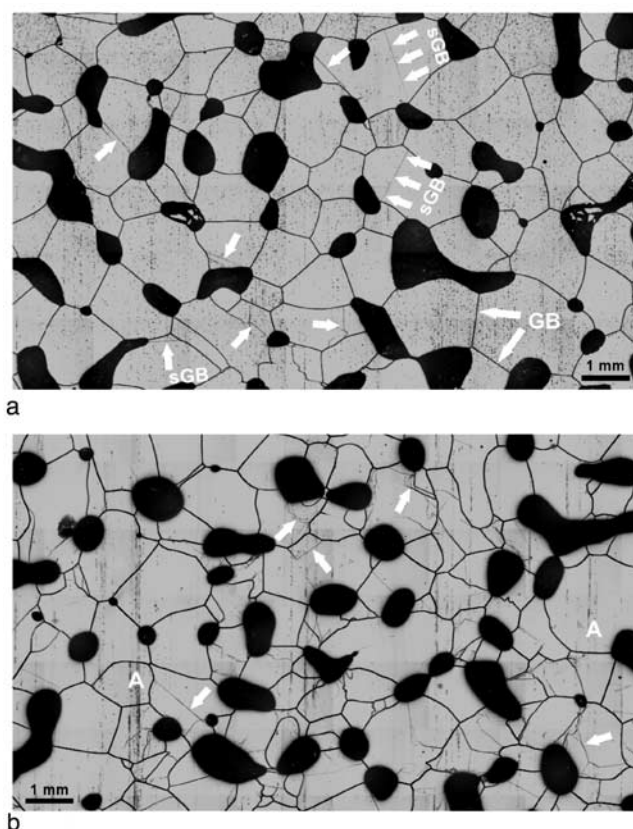


**Figure 2.** Microstructures from (a) 60 and (b) 80 m depths. The foam-type structure (Figure 2a) points to grain boundary migration driven by interface energy. The generation of a new grain structure with many intracrystalline deformation-related features (Figure 2b) is indicative for dynamic recrystallization. Gray is the ice matrix, and black is pores or bubbles and grain boundaries (some marked GB). The fainter gray lines inside the crystallites, often with open ends, are subgrain boundaries (shorter arrows; some marked sGB). Grain boundaries end in pores/bubbles or in triple junctions, i.e., where three grain boundaries meet. The fuzzy vertical stripes and dots are artifacts produced by microtoming (marked A). Shown are vertical sections of core B37; image dimensions are 13.2 mm  $\times$  8 mm.

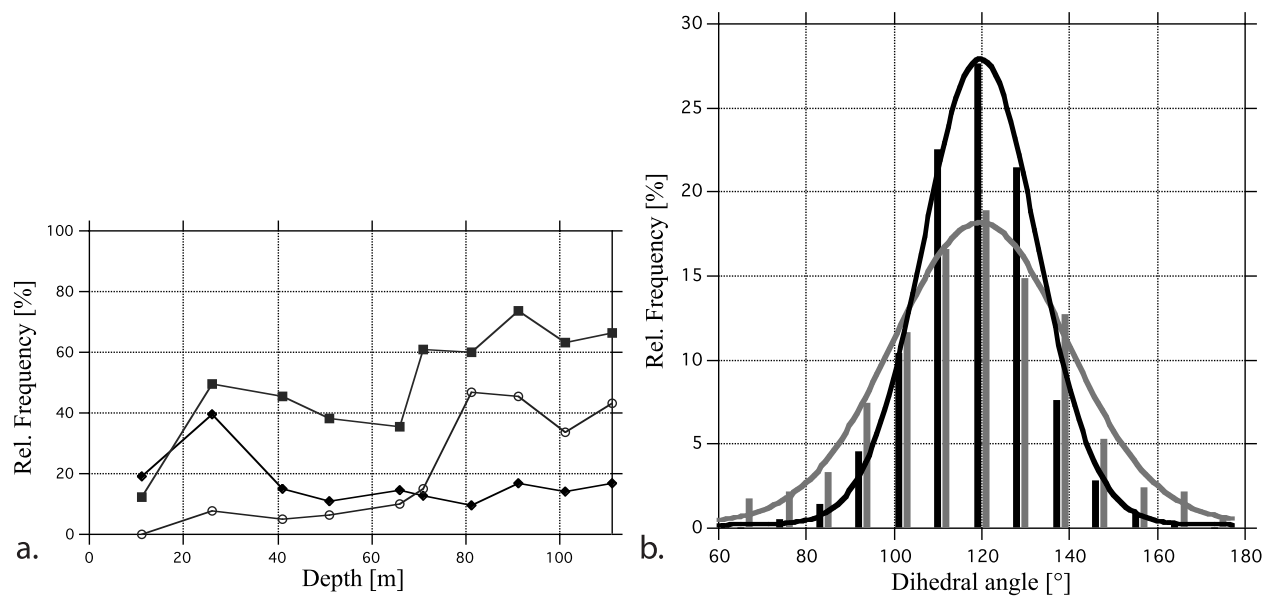


**Figure 3.** (a) Relative frequency of deformation-related microstructural features in grains versus depth. Squares, total number of grains showing deformation-related microstructural features. Diamonds, straight subgrain boundaries only. Open circles, straight and irregularly shaped subgrain boundaries. (b) Distribution of dihedral angles of the samples shown in Figure 2. Black, 60 m depth; gray, 80 m depth.

Figure 2b appears newly generated without any memory to its former structure indicating that a considerable volume fraction of the material has recrystallized. Any regularity of the original foam-like structure is absent. The grains are interlocking and the grain boundaries have irregular shapes. More grains exhibit deformation-related substructures (Figure 3a) and the distribution of the dihedral angles is broader (Figure 3b). The 80 m depth layer shows many relatively small grains not visible at 60 m depth. This is confirmed by the grain size distributions in Figure 4, which become broader with depth. Additionally, a considerably larger amount of small grains can be found in the samples from 85 and 105 m depths. The appearance of small grains correlates with an increase in the number of grains showing more complex intracrystalline substructures, viz. irregular subgrain boundaries appearing together with straight subgrain boundaries. An increased number of deformation-related features points to a more severe grain-grain interaction at densities higher than  $730 \text{ kg/m}^3$ .

[15] Figures 2, 3, and 4 consistently document the transition of the recrystallization regime from one driven by grain boundary energy to another one controlled by the inhomogeneous distribution of strain energy. The change in the aspect of the microstructure occurs in agreement with *Ebinuma et al.* [1985], who suggest that at the critical density of  $730 \text{ kg/m}^3$ , under an overburden snow load of about 0.2 MPa, firm has reached an optimum packing structure and dislocation creep is initiated.

[16] At this point it seems instructive to have a brief look at some typical microstructural features characteristic of dynamic recrystallization and how they develop with depth, density and time in Dronning Maud Land firm. In the high-porosity/low-density firm in the uppermost 40 m depth, straight subgrain boundaries (Figure 5) are the most frequent intracrystalline features. The straight subgrain boundaries probably originate from some sort of grain

subdivision process, like intracrystalline shear, bend or twist [*Bons and Jessell*, 1999; *Hamann et al.*, 2007; *Faria et al.*, 2009, also Is Antarctica like a birthday cake?, preprint 33/2006, Max Planck Institute for Mathematics in the Sciences, Leipzig, Germany, 2006, available at [http://www.mis.mpg.de/preprints/2006/preprint2006\\_33.pdf](http://www.mis.mpg.de/preprints/2006/preprint2006_33.pdf)]. Note the wedge-shaped grain in the grain at the lower left side showing multiple straight subgrain boundaries. One side is parallel to the bundle of straight subgrain boundaries indicating that new grains are already formed above 10 m depth by subdivision and rotation recrystallization. With decreasing porosity subdivision changes its character. In shallow depths at high porosity the grains are subdivided by one or few straight subgrain boundaries, which may develop to high-angle grain boundaries via rotation recrystallization. In deeper firm and typical for lower-porosity parts of grains often “split off” as shown in Figure 6. In extreme cases, a grating-type structure comes out, like in Figure 6b. These grains with a free corner preferentially form in the vicinity of triple junctions or pores. Figures 6c and 6d show that this special sort of subdivision can indeed produce new grains in firm. We assume that this is one process contributing to the population of small grains which emerge in the grain size distribution below 60 m depth (Figure 4). The mechanism of formation of such corner-type subgrain boundaries is still uncertain and needs further investigations.

[17] Bundles of straight subgrain boundaries represent areas of high concentration of defects and dislocations. Worth noticing in Figure 5 is the small kink in the upper grain where faint straight subgrain boundaries hit the grain boundary. More conspicuous examples of interaction between grain and subgrain boundaries are shown in Figure 7. As the region at the concave side of the bulging grain boundaries is free of any deformation-related features we can conclude that it was swept by the migrating grain boundary via  $\text{SIBM}_O$ . To assume that the grain boundaries

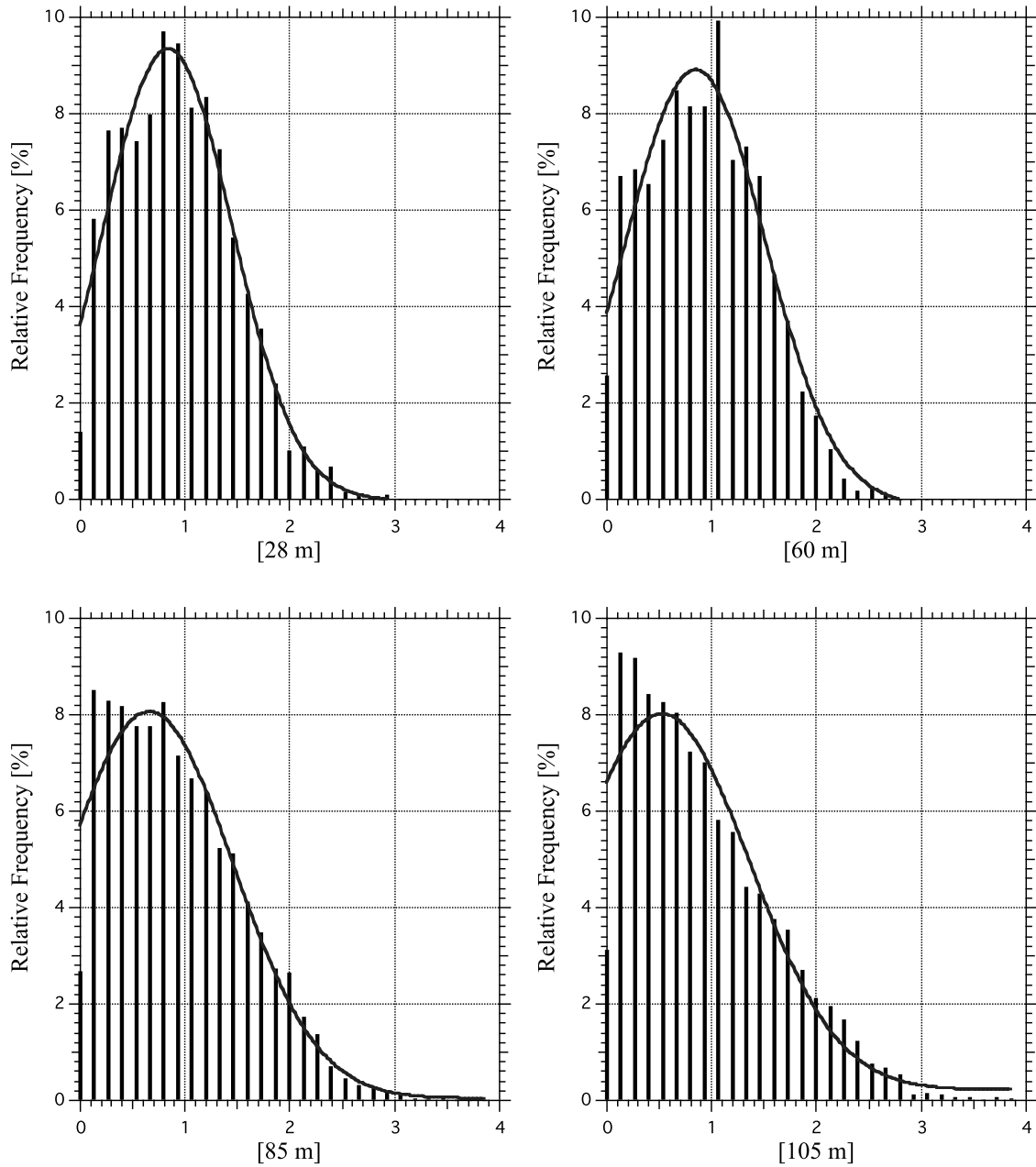


**Figure 4.** Distributions of equivalent grain radius at 28, 60, 85, and 105 m depths normalized by the average grain radius. A normal distribution has been fitted to each of the histograms.

migrate in the opposite direction away from the straight subgrain boundaries and generate the bundles is not realistic. Knowing the radius  $r$  at the tip of the bulging boundaries (equivalent radius: 43 and 55  $\mu\text{m}$ ) the driving force can be estimated by

$$\Delta E = 2\gamma/r, \quad (2)$$

where  $\gamma$  is the grain boundary energy (0.065  $\text{J}/\text{m}^2$ ) [e.g., *De La Chapelle et al.*, 1998]. The grain boundary energy is of the order of 3.0 and 2.3  $\text{kJ}/\text{m}^3$ , respectively. A lower bound of the dislocation density  $\rho$  is estimated from

$$E = \rho G b^2 / 2, \quad (3)$$

where  $G$  is the shear modulus ( $3 \times 10^9$  Pa) and  $b$  the Burger vector ( $4.5 \times 10^{-10}$  m) [*De La Chapelle et al.*, 1998]. The curvatures of the two bulging grain boundaries in Figure 7 convert into a dislocation density of ca.  $10^{13} \text{m}^{-2}$ . This value is about 2 orders of magnitude larger than the mean dislocation density calculated for the GRIP and Vostok ice cores [*De La Chapelle et al.*, 1998] and may explain the interaction between the grain boundaries and the straight subgrain boundaries (see kinks where single subgrain boundaries meet the two grain boundaries in Figure 7a). The compaction of the porous firm provides the energy necessary to produce these high dislocation densities and to initiate subdivision and SIBM in the upper firm column, in which ca. 40% of all grains contain intracrystalline features

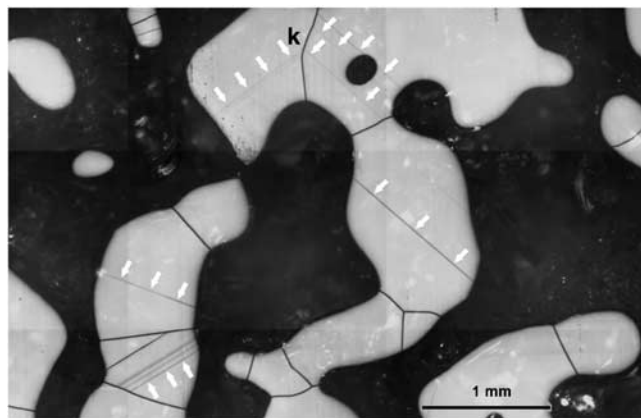


**Figure 5.** Straight subgrain boundaries (marked by white arrows), the most peculiar microstructural feature of polar firn close to the ice sheet surface. Kinks resulting from grain-subgrain boundary interaction are marked by k. Shown is a horizontal section of core B35 with depth 8 m.

related to deformation (Figure 3a). Localization of the deformation in the grains as observed in Figures 5 and 7 seems an important feature. That SIBM becomes more important with depth is easy to explain by the increase in the overburden snow load. At densities of about  $730 \text{ kg/m}^3$  the stored strain energy in many grains is so high that a combination of localized grain boundary bulging and subsequent subgrain rotation (viz. nucleation recrystallization, or SIBM<sub>N</sub>) leads to the formation of new grains, a process well known in metals and minerals [Beck and Sperry, 1950; Bailey and Hirsch, 1962; Wilson, 1982; Urai

*et al.*, 1986]. The formation of two-sided grains, grains with only two neighbors, is closely related to localized bulging of grain and subgrain boundaries, as demonstrated in Figure 8. This sequence of images shows different stages of development of two-sided grains, and it suggests that several mechanisms are active for the production of such new grains.

[18] At the end of our microstructural analysis we have to mention the issue of temperature. Low temperatures have been a strong argument against dynamic recrystallization in the colder parts of an ice sheet, as it is assumed that rapid migration of grain boundaries between dislocation-free nuclei and deformed grains can occur only at temperatures higher than ca.  $-10^\circ\text{C}$  [Pimienta and Duval, 1989; Duval and Castelnau, 1995; De La Chapelle *et al.*, 1998]. While this argument seems to be true for ice deformed in laboratory, the microstructural features characteristic of dynamic recrystallization are typical of firn in Dronning Maud Land with an annual mean temperature of about  $-45^\circ\text{C}$ . Temperature can obviously not be a crucial parameter for the onset of dynamic recrystallization in polar firn.

### 3.3. Consequences for Grain Growth in Firn

[19] Grain growth is by definition the increase of the average grain size with time. Mathematically the two-dimensional average grain size is clearly defined as the sample's section area divided by the number of grains in the section, but in practice grain size measurements frequently do not follow such a trivial definition. A brief overview about the various methods applied for estimating the average grain size of ice core sections is given by Durand *et al.* [2006]. In the work by Gow [1969], which is probably the most cited study of grain growth in polar firn, the average grain size is derived from the 50 largest grains of sections

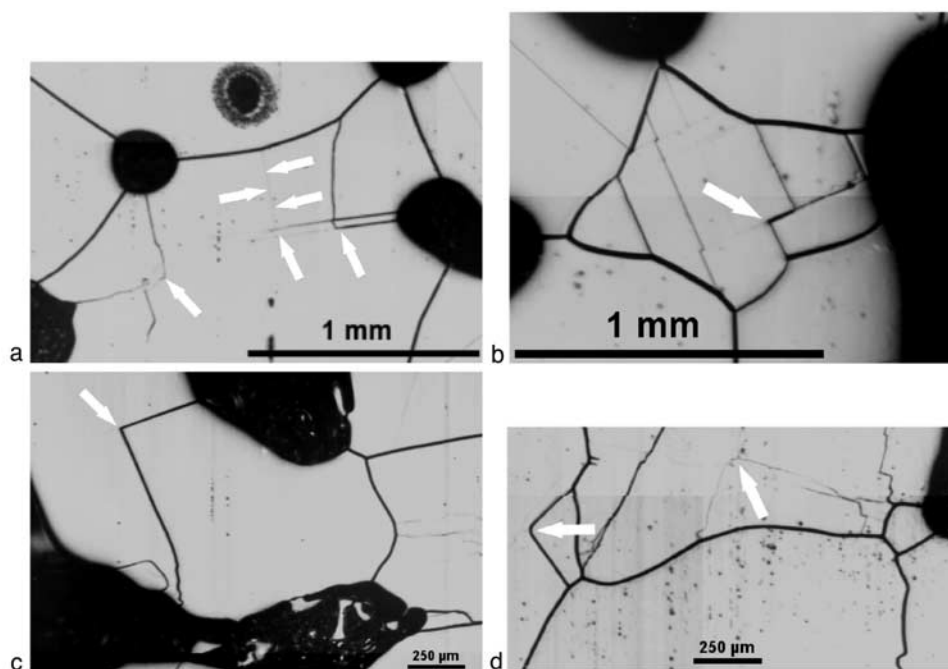


**Figure 6.** Corner-type subgrains and grains (marked by white arrows) (a and b) in development, (c) in a fully developed stage, and (d) in development (right arrow) and in a fully developed stage (left arrow). Shown are vertical sections of core B37 with depths 60 (Figures 6a, 6c, and 6d) and 70 m (Figure 6b).

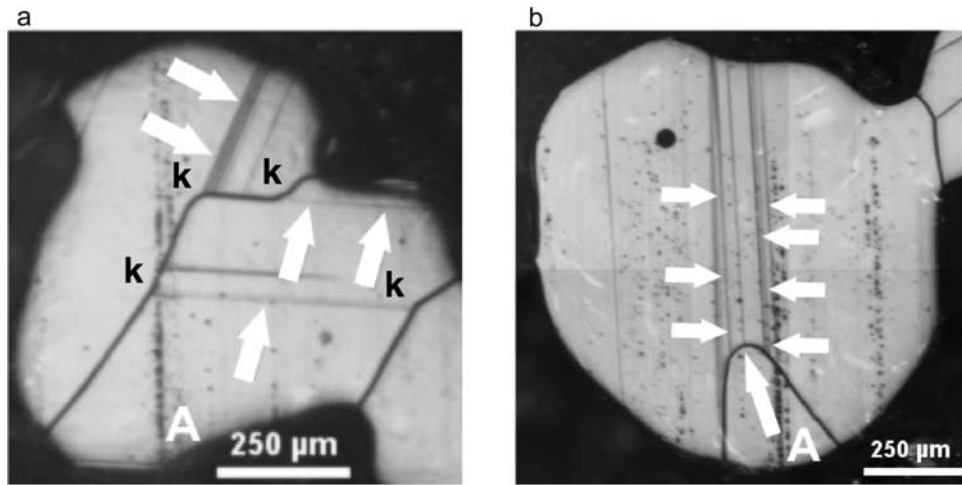


**Figure 7.** Evidence of  $SIBM_O$  (strain-induced boundary migration) close to the surface: grain-subgrain boundary interaction at (a) 1.3 and (b) 8.3 m. The grain boundaries bulge toward the bundles of subgrain boundaries. Short white arrows mark subgrain boundaries, the long arrow in Figure 7b marks the bulging grain boundary. As in Figure 2, the “greasy” and dotted vertical lines are artifacts from microtoming. Kinks resulting from grain-subgrain boundary interaction are marked by k. Shown are horizontal sections of core B35.

measuring  $1.75\text{ cm} \times 1.25\text{ cm}$ . The 50 largest grains only, which usually constitute ca. 25% of the total number of grains in such sections, were believed to yield a more realistic value than that based on measurements of all crystallites in a section, or a random selection. As pointed out by Durand *et al.* [2006], Gow’s method is not representative for the complete population. Until recently, most grain size data were determined manually. Today grain size

and c axis orientations are generally derived by applying image processing procedures on digital images of thin sections taken between crossed polarizers (for details see Durand *et al.* [2006]). Microstructure mapping belongs to this category of methods but differs in a few aspects. It is applied on mechanically stable thick sections of firm and has microscopic resolution. The main difference is however that grain boundaries are derived from their etch/sublimation

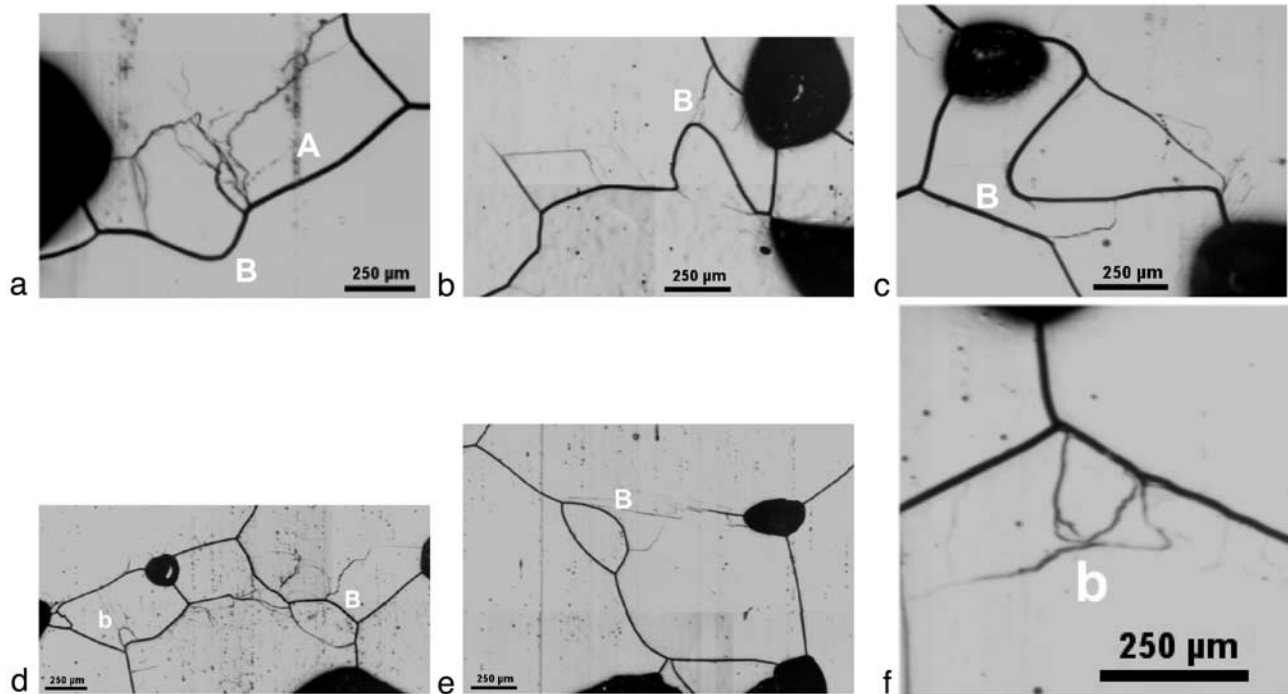


**Figure 8.** Evidence of  $SIBM_N$ : bulging grain (B) and subgrain (b) boundaries, a common structural phenomenon below 60 m depth. Some of these may give rise to two-sided grains. Shown are vertical sections of core B37 with depths (a, e, and f) 60 and (b, c, and d) 80 m.

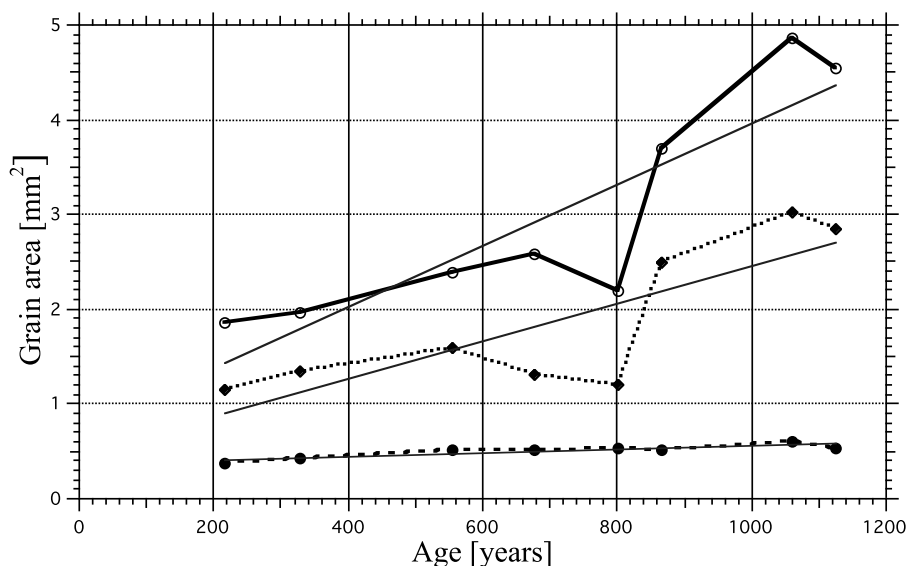


**Figure 9.** Average grain area versus age of the 100 (open circles) and 500 largest grains (diamonds) and all grains (closed circles) for the firn cores B35, B36, and B37.

grooves on a single plane, the cutting plane. This greatly improves the precision of the grain boundary measurements, as it limits the smallest grain size to the smallest area enclosed by a grain boundary loop, theoretically one pixel or  $13 \mu\text{m}$ . As the width of a grain boundary is also at least one pixel we have chosen a cutoff grain area of 20 pixels equivalent to a diameter of a circular area of about  $65 \mu\text{m}$ . Smaller grain areas are difficult to distinguish from noise produced by image processing. In comparison, the minimum grain size derived from thin sections is of the order of the thickness of the sections, about  $300\text{--}600 \mu\text{m}$ . From the mosaic images produced by microstructure mapping the vast majority of grain boundaries are identified unambiguously, only faint grain boundaries are not always easy to discriminate from subgrain boundaries. However, this difficulty is not a severe restriction as the resulting error is random; that is, it is unbiased with respect to grain or subgrain.

[20] Average grain sizes of sections determined from all crystals larger than  $65 \mu\text{m}$  (20 pixels) in diameter versus age are presented in Figure 9. Also included for comparison are the averages derived from the 100 and 500 largest firn crystals. As expected the 100 largest grains grow with time and so the averages of the largest 500 grains but the averages including all grains of a section do not show significant growth. They do practically not increase at all (from about  $0.4 \text{ mm}^2$  to  $0.5 \text{ mm}^2$ ) while the averages of the 100 and 500 largest grains more than double their size in the same time. This result is at first sight perplexing and needs further discussion, since it tells us that the average grain size depends strongly on the estimation method. This may in turn have severe consequences for the conclusions derived in the past concerning the dominating driving forces for grain boundary migration and the recrystallization regimes in polar firn.

[21] To illustrate how ambiguous the average grain size is when based on a special population of grains, we have calculated how the number of largest grains in a section

affects the average. Figure 10 demonstrates the dilemma that emerges independently of depth when only a limited number of the largest grains is chosen. The main result of Figure 10 is that there is no best number representative of the average grain size except the average over all: neither 50 nor any other number seems justified. Therefore, all grains of a section we can identify with high confidence must be considered when computing the average grain size. An arbitrarily selected population does not guarantee that the behavior of the deforming polycrystalline material is described well.

[22] Vanishing grain growth means that for a given area or volume the number of grains remains constant with time (or depth, in the case of ice cores) and that any disappearing grain must be counterbalanced by a new grain produced either by nucleation or subgrain rotation. Furthermore, the increase in size of the largest grains must be compensated by an equivalent increase in the number of grains smaller than the mean value. This behavior is well manifested in the grain size distribution in Figure 4. The number of small grains increases in the deeper sections and indicates a nonstationary grain size distribution, not compatible with normal grain growth. It must be emphasized that the growth of the largest grains does not imply that a few grains grow forever. As in deeper ice [Hamann *et al.*, 2009] larger grains tend to contain more deformation-related microstructural features than small grains. Obviously, some grains grow fast, deform fast and decompose into smaller grains via rotation recrystallization or nucleation. Grain growth and grain size reduction balance each other in a state of dynamic equilibrium. To summarize, vanishing grain growth, nonstationary grain size distributions and microstructural features characteristic of dynamic recrystallization are all evidences against the concept of normal grain growth. This study reports for the first time vanishing grain growth in firn from a site on a polar plateau. There is no physical or climatological reason to suppose that Dronning Maud Land firn could be exceptional. Therefore, we assume that the

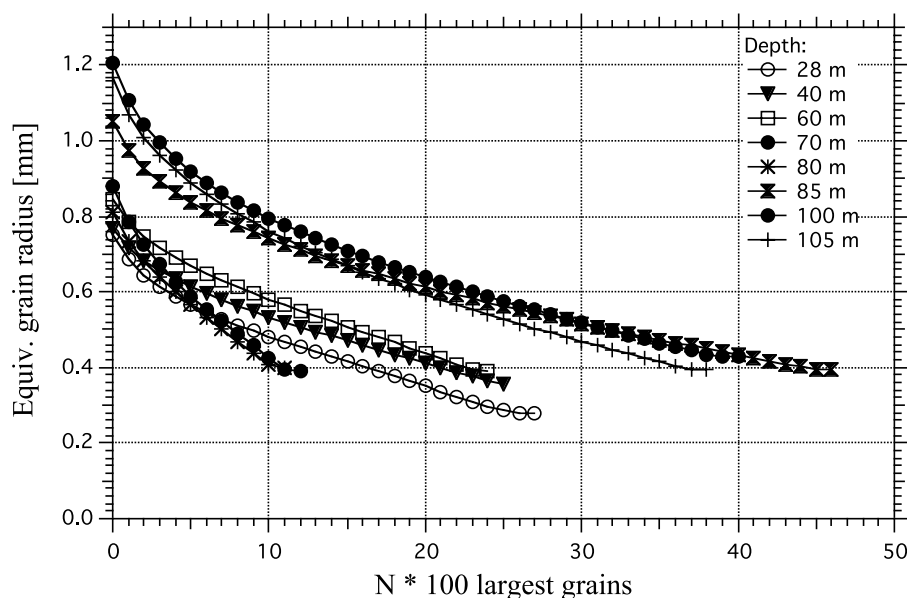


**Figure 10.** How to define a representative average grain size? Average equivalent grain radius versus number of largest grains included in the average ( $N$  times 100 largest grains) for different depths. Dimensions of the samples used for the grain size analysis:  $\sim 3 \text{ cm} \times 5 \text{ cm}$  at 70 and 80 m depths;  $\sim 5 \text{ cm} \times 5 \text{ cm}$  at 28, 40, and 60 m depths; and  $\sim 5 \text{ cm} \times 9 \text{ cm}$  at 85, 100, and 105 m depths.

disagreement with the results and conclusions of previous studies is related to the high resolution of our grain size data. Only the microscopic resolution enables us to identify grains as small as about  $65 \mu\text{m}$  in diameter and to study the behavior of such small grains. Our results lead to the conclusion that the concept of normal grain growth should not be applied to polar ice (and possibly also some other slowly deforming rocks). As remarked by *Faria and Hutter* [2001], numerical models based on the concept of normal grain growth may mimic the grain size profiles, but they do not explain the real physics. Our and other recent studies [*Mathiesen et al.*, 2004; *Durand et al.*, 2008] show the formation of new grains already occurs in firn and shallow ice, respectively.

#### 4. Conclusions

[23] Microstructural and grain size analyses of Dronning Maud Land firn have consistently shown that basic assumptions previously made to describe grain growth in polar firn and shallow ice as result of a normal grain growth process have to be questioned. Averages of the grain size derived from a limited number of grains do not reveal the true growth kinetics. A wide variety of microstructural features demonstrate that stored strain energy in firn is not at all small compared to the energy of the grain boundaries and temperature is not as important for dynamic recrystallization as previously thought. In particular, close to the firn-ice transition (density  $> 730 \text{ kg/m}^3$ ; overburden snow load  $\sim 0.2 \text{ MPa}$ ) the strain energy is so high that it rapidly modifies the entire grain structure, that is, at the firn-ice transition any memory of the original foam-like grain boundary structure is lost. Only dynamic recrystallization can explain the complete obliteration of one grain structure and generation of a new one within less than 400 years. Vanishing grain growth indicates a balance between grain

growth and grain size reduction. A more thorough discussion of grain growth in slowly deforming porous firn and polycrystalline ice seems indispensable. The discovery of dynamic recrystallization in firn and shallow ice demands a review of the deformation and recrystallization processes in the so-called “normal grain growth regime” of polar ice sheets.

[24] A deficit of this study is the missing information about the lattice orientations of the grains and subgrains resulting from bulging and involved in subdivision. Automated  $c$  axes measurements, EBSD and Laue diffraction studies shall be helpful to better characterize deformation-related structures on the grain scale in the near future.

[25] **Acknowledgments.** This work is a contribution to the European Project for Ice Coring in Antarctica (EPICA), a joint European Science Foundation/European Commission scientific program, funded by the EU (EPICA-MIS) and by national contributions from Belgium, Denmark, France, Germany, Italy, Netherlands, Norway, Sweden, Switzerland, and the United Kingdom. The main logistic support was provided by IPEV and PNRA (at Dome C) and AWI (at Dronning Maud Land). We thank P. Bons, C. Wilson, and an anonymous reviewer for helpful suggestions. The assistance of G. Stouf and K. Trimbom is gratefully acknowledged. The density profile was provided by H. Oerter. This is EPICA publication 219.

#### References

- Bailey, J. E., and P. B. Hirsch (1962), The recrystallization process in some polycrystalline metals, *Proc. R. Soc. London, Ser. A*, 267, 11–30, doi:10.1098/rspa.1962.0080.
- Beck, P. A., and P. R. Sperry (1950), Strain induced grain boundary migration in high purity aluminum, *J. Appl. Phys.*, 21, 150–152, doi:10.1063/1.1699614.
- Bons, P. D., and M. W. Jessell (1999), Micro-shear zones in experimentally deformed octachloropropane, *J. Struct. Geol.*, 21, 323–334, doi:10.1016/S0191-8141(98)90116-X.
- Burke, J. E. (1959), Grain growth in ceramics, in *Kinetics of High-Temperature Processes*, edited by W. D. Kingery, pp. 109–116, MIT Press, Cambridge, Mass.
- Cahn, R. W. (1974), Recovery and recrystallization, in *Physical Metallurgy*, edited by R. W. Cahn, pp. 1129–1197, North-Holland, Amsterdam.
- De La Chapelle, S., O. Castelnau, V. Lipenkov, and P. Duval (1998), Dynamic recrystallization and texture development in ice as revealed

- by the study of deep ice cores in Antarctica and Greenland, *J. Geophys. Res.*, *103*, 5091–5106, doi:10.1029/97JB02621.
- Durand, G., O. Gagliardini, T. Thorsteinsson, A. Svensson, J. Kipfstuhl, and D. Dahl-Jensen (2006), Ice microstructure and fabric: An up to date approach for measuring textures, *J. Glaciol.*, *52*, 619–630, doi:10.3189/172756506781828377.
- Durand, G., A. Persson, D. Samyn, and A. Svensson (2008), Relation between neighbouring grains in the upper part of the NorthGRIP ice core—Implications for rotation recrystallization, *Earth Planet. Sci. Lett.*, *265*, 666–671, doi:10.1016/j.epsl.2007.11.002.
- Duval, P. (1985), Grain growth and mechanical behaviour of polar ice, *Ann. Glaciol.*, *6*, 79–82.
- Duval, P., and O. Castelnau (1995), Dynamic recrystallization of ice in polar ice sheets, *J. Phys. IV*, *5*, 197–205.
- Ebinuma, T., H. Nishimura, N. Maeno, and S. Kawaguchi (1985), A new explanation of bending of a snow density profile, *Mem. Natl. Inst. Polar Res. Spec. Issue Jpn.*, *39*, 184–188.
- EPICA Community Members (2006), One-to-one coupling of glacial climate variability in Greenland and Antarctica, *Nature*, *444*, 195–198, doi:10.1038/nature05301.
- Faria, S. H., and K. Hutter (2001), The challenge of polycrystalline ice dynamics, in *Advances in Thermal Engineering and Sciences for Cold Regions*, edited by S. Kim and D. Jung, pp. 3–31, Soc. of Air Cond. and Refrigerating Eng. of Korea, Seoul.
- Faria, S. H., S. Kipfstuhl, N. Azuma, J. Freitag, I. Hamann, M. M. Murshed, and W. F. Kuhs (2009), The multiscale structure of the Antarctic ice sheet. Part I: Inland ice, in *Physics of Ice Core Records*, vol. 2, edited by T. Hondo, Hokkaido Univ. Press, Sapporo, Japan, in press.
- Goldsby, D. L., and D. L. Kohlstedt (2001), Superplastic deformation of ice: Experimental observations, *J. Geophys. Res.*, *106*, 11,017–11,030, doi:10.1029/2000JB900336.
- Gow, A. J. (1969), On the rates of growth of grains and crystals in south polar firm, *J. Glaciol.*, *8*, 241–252.
- Gow, A. J., and T. Williamson (1976), Rheological implications of the internal structure and crystal fabrics of the West Antarctic ice sheet as revealed by deep core drilling at Byrd Station, *Geol. Soc. Am. Bull.*, *87*(12), 1665–1677, doi:10.1130/0016-7606(1976)87<1665:RIOTIS>2.0.CO;2.
- Hamann, I., C. Weikusat, and N. Azuma (2007), Evolution of ice crystal microstructures during creep experiments, *J. Glaciol.*, *53*, 479–489, doi:10.3189/002214307783258341.
- Hamann, I., S. Kipfstuhl, S. H. Faria, and N. Azuma (2009), Sub-grain boundaries in EPICA Dronning Maudland (EDML) deep ice core, *J. Glaciol.*, in press.
- Humphreys, F. J., and M. Hatherly (2004), *Recrystallization and Related Annealing Phenomena*, 615 pp., Elsevier, Amsterdam.
- Kipfstuhl, S., I. Hamann, A. Lambrecht, J. Freitag, S. H. Faria, D. Grigoriev, and N. Azuma (2006), Microstructure mapping: A new method for imaging deformation induced microstructural features of ice on the grain scale, *J. Glaciol.*, *52*, 398–406, doi:10.3189/172756506781828647.
- Liboutry, L., and P. Duval (1985), Various isotropic and anisotropic ices found in glaciers and polar ice caps and their corresponding rheologies, *Ann. Geophys., Ser. B*, *3*, 207–224.
- Maeno, N., and T. Ebinuma (1983), Pressure sintering of ice and its implication to the densification of snow at polar glaciers and ice sheets, *J. Phys. Chem.*, *87*(21), 4103–4110, doi:10.1021/j100244a023.
- Mathiesen, J., J. Ferkinghoff-Borg, M. H. Jensen, M. Levinsen, P. Olesen, D. Dahl-Jensen, and A. Svensson (2004), Dynamics of crystal formation in the Greenland NorthGRIP ice core, *J. Glaciol.*, *50*, 325–328, doi:10.3189/172756504781829873.
- Pan, J. Z. (2003), Modelling sintering at different length scales, *Int. Mater. Rev.*, *48*(2), 69–85, doi:10.1179/095066002225010209.
- Pimienta, P., and P. Duval (1989), Rheology of polar glacier ice, *Ann. Glaciol.*, *12*, 206–207.
- Rice, R. W. (1998), *Porosity of Ceramics*, Marcel Dekker, New York.
- Stephenson, P. J. (1967), Some considerations of snow metamorphism in the Antarctic ice sheet in the light of ice crystal studies, in *Physics of Snow and Ice*, vol. 1, edited by H. Oura, pp. 725–740, Inst. of Low Temp. Sci., Sapporo, Japan.
- Urai, J. L., W. D. Means, and G. S. Lister (1986), Dynamic recrystallization of minerals, in *Mineral and Rock Deformation: Laboratory Studies*, *Geophys. Monogr. Ser.*, vol. 36, edited by B. E. Hobbs and H. C. Heard, pp. 213–232, AGU, Washington, D. C.
- Vischer, N. O. E., P. G. Huls, and C. L. Woldringh (1994), Object-image: An interactive image analysis program using structured point collection, *Binary*, *6*, 160–166.
- Wilkinson, D. S., and M. F. Ashby (1975), Pressure sintering by power law creep, *Acta Metall.*, *23*(11), 1277–1285, doi:10.1016/0001-6160(75)90136-4.
- Wilson, C. J. L. (1982), Texture and grain growth during the annealing of ice, *Textures Microstruct.*, *5*, 19–31, doi:10.1155/TSM.5.19.
- Wilson, C. J. L. (1986), Deformation induced recrystallization of ice: The application of in situ experiments, in *Mineral and Rock Deformation: Laboratory Studies*, *Geophys. Monogr. Ser.*, vol. 36, edited by B. E. Hobbs and H. C. Heard, pp. 213–232, AGU, Washington, D. C.

N. Azuma, Department of Mechanical Engineering, Nagaoka University of Technology, 16031 Kamitomioka, Nagaoka, 940-2188 Niigata, Japan.

S. H. Faria, Section of Crystallography, GZG, University of Göttingen, Goldschmidtstrasse 1, D-37077 Göttingen, Germany.

J. Freitag, I. Hamann, S. Kipfstuhl, H. Miller, and F. Wilhelms, Alfred Wegener Institute for Polar and Marine Research, Columbusstrasse, D-27568 Bremerhaven, Germany. (sepp.kipfstuhl@awi.de)

P. Kaufmann and K. Weiler, Climate and Environmental Physics, Physics Institute, University of Bern, Sidlerstrasse 5, CH-3012 Bern, Switzerland.